

1 **Detecting small-scale spatial heterogeneity and temporal dynamics of soil organic carbon**
2 **(SOC) stocks: a comparison between automatic chamber-derived C budgets and repeated**
3 **soil inventories**

4
5 Mathias Hoffmann^{a,*}, Nicole Jurisch^b, Juana Garcia Alba^a, Elisa Albiac Borraz^a, Marten
6 Schmidt^b, Vytas Huth^b, Holger Rogasik^a, Helene Rieckh^a, Gernot Verch^c, Michael Sommer^{a, d},
7 Jürgen Augustin^b

8
9 ^aInstitute of Soil Landscape Research, Leibniz Centre for Agricultural Landscape Research
10 (ZALF), Eberswalder Str. 84, 15374 Müncheberg, Germany

11 ^bInstitute of Landscape Biogeochemistry, Leibniz Centre for Agricultural Landscape Research
12 (ZALF), Eberswalder Str. 84, 15374 Müncheberg, Germany

13 ^cResearch Station Dedelow, Leibniz Centre for Agricultural Landscape Research (ZALF),
14 Eberswalder Str. 84, 15374 Müncheberg, Germany

15 ^dInstitute of Earth and Environmental Sciences, University Potsdam, Karl-Liebknecht-Str.24-25,
16 14476 Potsdam, Germany

17
18 *Corresponding author:

19 Mathias Hoffmann

20 Eberswalder Str. 84, 15374 Müncheberg, Germany

21 E-mail: Mathias.Hoffmann@zalf.de

22 Tel.: +49(0)33432 82 327

23 Fax: +49(0)33432 82 280

24 **Abstract**

25 Carbon (C) sequestration in soils plays a key role in the global C cycle. It is therefore crucial to
26 adequately monitor dynamics in soil organic carbon (Δ SOC) stocks when aiming to reveal
27 underlying processes and potential drivers. However, small-scale spatial (10-30 m) and temporal
28 changes in SOC stocks, particularly pronounced on arable lands, are hard to assess. The main
29 reasons for this are limitations of the well-established methods. On the one hand, repeated soil
30 inventories, often used in long-term field trials, reveal spatial patterns and trends in Δ SOC but
31 require a longer observation period and a sufficient number of repetitions. On the other hand,
32 eddy covariance measurements of C fluxes towards a complete C budget of the soil-plant-
33 atmosphere system may help to obtain temporal Δ SOC patterns but lack small-scale spatial
34 resolution.

35 To overcome these limitations, this study presents a reliable method to detect both short-term
36 temporal dynamics as well as small-scale spatial differences of Δ SOC. Therefore, a combination
37 of automatic chamber (AC) measurements of CO₂ exchange and empirically modeled
38 aboveground biomass development (NPP_{shoot}) was used. To verify our method, results were
39 compared with Δ SOC observed by soil resampling.

40 Soil resampling and AC measurements were performed from 2010 to 2014 at a colluvial
41 depression located in the hummocky ground moraine landscape of NE Germany. The
42 measurement site is characterized by a variable groundwater level (GWL) and pronounced small-
43 scale spatial heterogeneity regarding SOC and nitrogen (Nt) stocks. . Tendencies and magnitude
44 of Δ SOC values derived by AC-measurements and repeated soil inventories corresponded well.
45 The period of maximum plant growth was identified as being most important for the development
46 of spatial differences in annual Δ SOC. Hence, we were able to confirm that AC-based C budgets
47 are able to reveal small-scale spatial differences and short-term temporal dynamics of Δ SOC.

48

49 **Keywords**

50 Net ecosystem exchange (NEE), net primary productivity (NPP), biomass modeling, soil

51 resampling

52

53 **1. Introduction**

54 Soils are the largest terrestrial reservoirs of organic carbon (SOC), storing two to three times as
55 much C as the atmosphere and biosphere (Chen et al., 2015; Lal et al., 2004). In the context of
56 climate change mitigation as well as soil fertility and food security, there has been considerable
57 interest in the development of SOC, especially in erosion-affected agricultural landscapes (Berhe
58 and Kleber, 2013; Conant et al., 2011; Doetterl et al., 2016; Stockmann et al., 2015; Van Oost et
59 al., 2007; Xiong et al., 2016). Detecting the development of soil organic carbon stocks (Δ SOC) in
60 agricultural landscapes needs to consider three major challenges: First, the high small-scale
61 spatial heterogeneity of SOC (e.g., Conant et al., 2011; Xiong et al., 2016). Erosion and land use
62 change reinforce natural spatial and temporal variability, especially in hilly landscapes such as
63 hummocky ground moraines where correlation lengths in soil parameters of 10-30 m are very
64 common. Second, pronounced short-term temporal dynamics, caused by, e.g., type of cover crop,
65 frequent crop rotation and soil cultivation practices. Third, the rather small magnitude of Δ SOC
66 compared to total SOC stocks (e.g., Conant et al., 2011; Poeplau et al., 2016).

67 However, information on the development of SOC is an essential precondition to improve the
68 predictive ability of terrestrial C models (Luo et al., 2014). As a result, sensitive measurement
69 techniques are required to precisely assess short-term temporal and small-scale (10-30 m) spatial
70 dynamics in Δ SOC (Batjes and van Wesemael, 2015). To date, the assessment of Δ SOC is
71 typically based on two methods, namely (i) destructive, repeated soil inventories through soil
72 resampling and (ii) non-destructive determination of ecosystem C budgets by measurements of
73 gaseous C exchange, C import and C export (Leifeld et al., 2011).

74 The first method is usually used during long-term field trials (Batjes and van Wesemael, 2015;
75 Chen et al., 2015; Schrumpf et al., 2011). Given a sufficient time horizon of 5 to 10 years, the
76 soil resampling method is generally able to reveal spatial patterns and trends within Δ SOC

77 (Batjes and van Wesemael, 2015; Schrumpf et al., 2011). Most repeated soil inventories are
78 designed to study treatment differences in the long-term. As a result, short-term temporal
79 dynamics in C exchange remain concealed (Poeplau et al., 2016; Schrumpf et al., 2011). A
80 number of studies tried to overcome this methodical limitation by increasing (e.g., monthly) the
81 soil sampling frequency (Culman et al., 2013; Wuest, 2014). This allows for the detection of
82 seasonal patterns of Δ SOC but still mixes temporal and spatial variability of SOC because every
83 new soil sample represents not only a repetition in time but also in space. Temporal differences
84 observed through repeated soil sampling are therefore always spatially biased.

85 By contrast, the net ecosystem carbon budget (NECB; Smith et al. 2010) and thereon based
86 temporal dynamics of Δ SOC can be easily derived through the eddy covariance (EC) technique
87 as a common approach to obtain gaseous C exchange (Alberti et al., 2010; Leifeld et al., 2011;
88 Skinner and Dell, 2015). However, C fluxes based on EC measurements are integrated over a
89 larger, altering footprint area (several hectares). As a result, small-scale (< 20 m) spatial
90 differences in Δ SOC are not detected.

91 Accounting for the above-mentioned methodical limitations, a number of studies investigated
92 spatial patterns in gaseous C exchange by using manual chamber measurement systems
93 (Eickenscheidt et al., 2014; Pohl et al., 2015). Compared to EC measurements, these systems are
94 characterized by a low temporal resolution, where the calculated net ecosystem CO₂ exchange
95 (NEE) is commonly based on extensive gap filling (Gomez-Casanovas et al., 2013; Savage and
96 Davidson, 2003) conducted, e.g., using empirical modeling (Hoffmann et al., 2015). Therefore,
97 management practices and different stages in plant development that are needed to precisely
98 detect NEE often remain unconsidered (Hoffmann et al., 2015).

99 Compared to mentioned approaches for detecting Δ SOC by either repeated soil sampling or
100 observations of the gaseous C exchange, automatic chamber (AC) systems combine several

101 advantages. On the one hand flux measurements of the same spatial entity avoid the mixing of
102 spatial and temporal variability, as done in case of point measurements by repeated soil
103 inventories. On the other hand, AC measurements combine advantages of EC and manual
104 chamber systems because they not only increase the temporal resolution compared to manual
105 chambers but also allow for the detection of small-scale spatial differences and treatment
106 comparisons regarding the gaseous C exchange (Koskinen et al., 2014).

107 To date hardly any direct comparisons between AC-derived C budgets and soil resampling-based
108 Δ SOC values have been reported in the literature. Leifeld et al. (2011) and Verma et al. (2005)
109 compared the results of repeated soil inventories with EC-based C budgets over 5- and 3-year
110 study periods, respectively. Even though temporal dynamics in Δ SOC were shown e.g. for grazed
111 pastures and intensively used grasslands (Skinner and Dell 2015; Leifeld et al., 2011), no attempt
112 was made to additionally detect small-scale differences in Δ SOC. In our study, we introduce the
113 combination of AC measurements and empirically modeled aboveground biomass production
114 (NPP_{shoot}) as a precise method to detect small-scale spatial differences and short-term temporal
115 dynamics of Δ SOC. Measurements were performed from 2010 to 2014 under a *silage*
116 *maize/winter fodder rye/sorghum-Sudan grass hybrid/alfalfa* crop rotation at an experimental plot
117 located in the hummocky ground moraine landscape of NE Germany.

118 We hypothesize that the AC-based C budget method is able to detect small-scale spatial and
119 short-term temporal dynamics of Δ SOC in an accurate and precise manner. Therefore, we
120 compare Δ SOC values measured by soil resampling with Δ SOC values derived through AC-
121 based C budgets (Fig. 1).

122

123 **2. Materials and methods**

124 **2.1 Study site and experimental setup**

125 Measurements were performed at the 6-ha experimental field “CarboZALF-D”. The site is
126 located in a hummocky arable soil landscape within the Uckermark region (NE-Germany;
127 53°23`N, 13°47`E, ~50-60 m a.s.l.). The temperate climate is characterized by a mean annual air
128 temperature of 8.6°C and annual precipitation of 485 mm (1992–2012, ZALF research station,
129 Dedelow). Typical landscape elements vary from flat summit and depression locations with a
130 gradient of approximately 2 %, across longer slopes with a medium gradient of approx. 6 %, to
131 short and rather steep slopes with a gradient of up to 13 %. The study site shows complex soil
132 patterns mainly influenced by erosion, relief and parent material, e.g., sandy to marly glacial and
133 glaciofluvial deposits. The soil type inventory of the experimental site consists of non-eroded
134 Albic Luvisols (Cutanic) at the flat summits, strongly eroded Calcic Luvisols (Cutanic) on the
135 moderate slopes, extremely eroded Calcaric Regosols on the steep slopes, and a colluvial soil,
136 i.e., Endogleyic Colluvic Regosols (Eutric), over peat in the depression (IUSS Working Group
137 WRB, 2015).

138 During June 2010, four automatic chambers and a WXT520 climate station (Vaisala, Vantaa,
139 Finland) were set up at the depression (Sommer et al., 2016) (see 2.2.1). The chambers were
140 arranged along a topographic gradient (upper (A), upper middle (B), lower middle (C), and lower
141 (D) chamber position; length ~30 m; difference in altitude ~1 m) within in a distance of approx. 5
142 m of each other (Fig. 2). As part of the CarboZALF project, a manipulation experiment was
143 carried out at the end of October 2010, i.e., after the vegetation period. Topsoil material from a
144 neighboring hillslope was incorporated into the upper soil layer of the depression (Ap horizon).
145 The amount of translocated soil was equivalent to tillage erosion of a decennial time horizon
146 (Sommer et al., 2016). The change in SOC for each chamber was monitored by three topsoil
147 inventories, carried out (I) prior to soil manipulation during April 2009, (II) after soil
148 manipulation during April 2011, and (III) during December 2014. Δ SOC derived through soil

149 resampling and AC-based C budgets, was compared for the period between April 2011 and
150 December 2014 (Fig. 1).

151 Records of meteorological conditions (1 min frequency) include measurements of air temperature
152 at 20 cm and 200 cm height, PAR (inside and outside the chamber), air humidity, precipitation,
153 air pressure, wind speed and direction. Soil temperatures at depths of 2 cm, 5 cm, 10 cm and 50
154 cm were recorded using thermocouples, installed next to the climate station (107, Campbell
155 Scientific, UT, USA).

156 The groundwater level (GWL) was measured using tensiometers assuming hydrostatic
157 equilibrium. The tensiometers were installed at a soil depth of 160 cm, at soil profile locations in
158 the upper and lower end of the transect. The average GWL of both profiles was used for further
159 data analysis. Data gaps < 2 days were filled using simple linear interpolation. Larger gaps in
160 GWL did not occur. The measurement site was cultivated with five different crops during the
161 study period, following a practice-orientated and erosion-expedited farming procedure. The crop
162 rotation was silage maize (*Zea mays*) - winter fodder rye (*Secale cereale*) - sorghum-Sudan grass
163 hybrid (*Sorghum bicolor* x *sudanese*) - winter triticale (*Triticosecale*) - alfalfa (*Medicago sativa*).
164 Cultivation and fertilization details are presented in Tab. A.1. Aboveground biomass (NPP_{shoot})
165 development was monitored using up to four biomass sampling campaigns during the growing
166 season, covering the main growth stages. Additional measurements of leaf area index (LAI)
167 started in 2013. Collected biomass samples were chopped and dried to a constant weight (48 h at
168 105°C). The C, N, K and P contents were determined using elementary analysis (C, N: TruSpec
169 CNS analyzer, LECO Ltd., Mönchengladbach, Germany) and Kjehldahl digestion (P, K; AT200,
170 BeckmanCoulter (Olympus), Krefeld, Germany and AAS-iCE3300, ThermoFisher-SCIENTIFIC
171 GmbH, Darmstadt, Germany). To assess the potential impact of chamber placement on plant

172 growth, chemical analyses were carried out for the final harvests of each chamber and compared
173 to biomass samples collected next to each chamber.

174

175 **2.2 C budget method**

176 **2.2.1 Automatic chamber system**

177 Automatic flow-through non-steady-state (FT-NSS) chamber measurements (Livingston and
178 Hutchinson, 1995) of CO₂ exchange were conducted from January 2010 until December 2014.

179 The AC system consists of 4 identical, rectangular, transparent polycarbonate chambers
180 (thickness of 2 mm; light transmission ~70 %). Each chamber has a height of 2.5 m and covers a
181 surface area of 2.25 m² (volume: 5.625 m³). To adapt for plant height (alfalfa), the chamber
182 volume was reduced to 3.375 m³ in autumn 2013. Airtight closure during measurements was
183 ensured by a rubber belt that sealed at the bottom of each chamber. A 30-cm open-ended tube on
184 the slightly concave top of the chambers guided rain water into the chamber and additionally
185 assured pressure equalization. Two small axial fans (5.61 m³ min⁻¹) were used for mixing the
186 chamber headspace. The chambers were mounted onto steel frames with a height of 6 m and
187 lifted between measurements using electrical winches at the top. For controlling the AC system
188 and data collection, a CR1000 data logger was used (Campbell Scientific, UT, USA). The CO₂
189 concentration changes over time were measured within each chamber using a carbon dioxide
190 probe (GMP343, Vaisala, Vantaa, Finland) connected to a vacuum pump (0.001 m³ min⁻¹;
191 DC12/16FK, Fürgut, Tannheim, Germany). All CO₂ probes were calibrated prior to installation
192 using ± 0.5 % accurate gases containing 0 ppm, 200 ppm, 370 ppm, 600 ppm, 1000, ppm and
193 4000 ppm CO₂. The operation schedule of the AC system, decisively influenced by agricultural
194 treatments, is presented in A.2. The chambers closed in parallel at an hourly frequency, providing
195 one flux measurement per chamber and hour. The measurement duration was 5-20 minutes,

196 depending on season and time of day. Nighttime measurements usually lasted 10 min during the
197 growing season and 20 min during the non-growing season (due to lower concentration
198 increments). The length of the daytime measurements was up to 10 min, depending on low PAR
199 fluctuations (< 20 %). CO₂ concentrations (inside the chamber) and general environmental
200 conditions, such as PAR (SKP215, Skye, Llandridad Wells, UK) and air temperatures (107,
201 Campbell Scientific, UT, USA), were recorded inside and outside the chambers at a 1 min
202 frequency from 2010 to 2012 and a 15 sec frequency from October 2012.

203

204 **2.2.2 CO₂ flux calculation and gap filling**

205 An adaptation of the modular R program script, described in detail by Hoffmann et al. (2015),
206 was used for stepwise data processing. The atmospheric sign convention was used for the
207 components of gaseous C exchange (ecosystem respiration (R_{eco}; sum of autotrophic and
208 heterotrophic respiration), gross primary production (GPP) and NEE), whereas positive values
209 for ΔSOC indicate a gain and negative values a loss in SOC. Based on records of environmental
210 variables and CO₂ concentration change within the chamber headspace, CO₂ fluxes were
211 calculated and parameterized for R_{eco} and GPP within an integrative step. Subsequently, R_{eco},
212 GPP, and NEE were modeled for the entire measurement period using climate station data.
213 Statistical analyses, model calibration and comprehensive error prediction were provided for all
214 steps of the modeling process.

215 CO₂ fluxes (F , μmol C m⁻² s⁻¹) were calculated according to the ideal gas law (Eq. 1).

216

$$217 \quad F = \frac{pV}{RTA} * \frac{\Delta c}{\Delta t} \quad [Eq. 1]$$

218

219 where $\Delta c/\Delta t$ is the concentration change over measurement time, A and V denote the basal area
220 and chamber volume, respectively, and T and p represent the air temperature inside the chamber
221 (K) and air pressure. Because plants below the chambers accounted for < 0.2 % of the total
222 chamber volume, a static chamber volume was assumed. R is a constant ($8.3143 \text{ m}^3 \text{ Pa K}^{-1} \text{ mol}^{-1}$).
223 ¹). To calculate $\Delta c/\Delta t$, data subsets based on a variable moving window with a minimum length
224 of 4 minutes were used (Hoffmann et al., 2015). $\Delta c/\Delta t$ was computed by applying a linear
225 regression to each data subset, relating changes in chamber headspace CO₂ concentration to
226 measurement time (Leiber-Sauheitl et al., 2013; Leifeld et al., 2014; Pohl et al., 2015). In the case
227 of the 15-sec measurement frequency, a death-band of 5 % was applied prior to the moving
228 window algorithm. Thus, data noise that originated from either turbulence or pressure fluctuation
229 caused by chamber deployment or from increasing saturation and canopy microclimate effects
230 was excluded (Davidson et al., 2002; Kutzbach et al., 2007; Langensiepen et al., 2012). Due to
231 the low measurement frequency, no data points were discarded for records with 1-min
232 measurement frequency (2010-2012). The resulting CO₂ fluxes per measurement (based on the
233 moving window data subsets) were further evaluated according to the following exclusion
234 criteria: (i) range of within-chamber air temperature not larger than $\pm 1.5 \text{ K}$ (R_{eco} and NEE
235 fluxes) and a PAR deviation (NEE fluxes only) not larger than $\pm 20 \%$ of the average to ensure
236 stable environmental conditions within the chamber throughout the measurement; (ii) significant
237 regression slope ($p \leq 0.1$, *t*-test); and (iii) non-significant tests ($p > 0.1$) for normality (Lillifor's
238 adaption of the Kolmogorov-Smirnov test), homoscedasticity (Breusch-Pagan test) and linearity
239 of CO₂ concentration data. Calculated CO₂ fluxes that did not meet all exclusion criteria were
240 discarded. In cases where more than one flux per measurement met all exclusion criteria, the CO₂
241 flux with the steepest slope was chosen.

242 To account for measurement gaps and to obtain cumulative NEE values, empirical models were
 243 derived based on nighttime R_{eco} and daytime NEE measurements following Hoffmann et al.
 244 (2015). For R_{eco} , temperature-dependent Arrhenius-type models were used and fitted for recorded
 245 air as well as soil temperatures in different depths (Lloyd and Taylor 1994; Eq. 2).

$$247 \quad R_{eco} = R_{ref} * e^{E_0 \left(\frac{1}{T_{ref}-T_0} - \frac{1}{T-T_0} \right)} \quad [Eq. 2]$$

248
 249 where R_{eco} is the measured ecosystem respiration rate [$\mu\text{mol}^{-1} \text{C m}^{-2} \text{s}^{-1}$], R_{ref} is the respiration
 250 rate at the reference temperature (283.15 K; T_{ref}); E_0 is an activation energy like parameter; T_0 is
 251 the starting temperature constant (227.13 K) and T is the mean air or soil temperature during the
 252 flux measurement. Out of the four R_{eco} models (one model for air temperature, soil temperature in
 253 2 cm, 5 cm and 10 cm depth) obtained for nighttime R_{eco} measurements of a certain period, the
 254 model with the lowest Akaike Information Criterion (AIC) was used.

255 GPP fluxes were derived using a PAR-dependent, rectangular hyperbolic light response function
 256 based on the Michaelis-Menten kinetic (Elsgaard et al., 2012; Hoffmann et al., 2015; Wang et al.,
 257 2013; Eq. 3). Because GPP was not measured directly, GPP fluxes were calculated as the
 258 difference between measured NEE and modeled R_{eco} fluxes.

$$260 \quad GPP = \frac{GP_{max} * \alpha * PAR}{\alpha * PAR + GP_{max}} \quad [Eq. 3]$$

261
 262 where GPP is the calculated gross primary productivity [$\mu\text{mol}^{-1} \text{CO}_2 \text{m}^{-2} \text{s}^{-1}$]; GP_{max} is the
 263 maximum rate of C fixation at infinite PAR [$\mu\text{mol CO}_2 \text{m}^{-2} \text{s}^{-1}$]; α is the light use efficiency [mol
 264 $\text{CO}_2 \text{mol}^{-1}$ photons] and PAR is the photon flux density (inside the chamber) of the

265 photosynthetically active radiation [μmol^{-1} photons m^{-2} s^{-1}]. In cases where the rectangular
266 hyperbolic light response function did not result in significant parameter estimates, a non-
267 rectangular hyperbolic light-response function was used (Gilmanov et al. 2007, 2013; Eq. 4).

268

$$269 \quad GPP = \alpha * PAR + GP_{\max} - \sqrt{(\alpha * PAR + GP_{\max})^2 - 4 * \alpha * PAR * GP_{\max} * \theta} \quad [\text{Eq. 4}]$$

270

271 where θ is the convexity coefficient of the light-response equation (dimensionless).

272 Due to plant growth and season, parameters of derived R_{eco} and GPP models may vary with time.

273 To account for this, a moving window parameterization was performed, by applying fluxes of a

274 variable time window (2-21 consecutive measurement days) to Eq.2-4. Temporally overlapping

275 R_{eco} and GPP model sets were evaluated and discarded in case of positive (GPP), negative (R_{eco})

276 or insignificant parameter estimates. Finally, the model set with the lowest AIC (R_{eco}) was used.

277 If no fit or a non-significant fit was achieved, averaged flux rates were applied for R_{eco} and GPP.

278 The length of the averaging period was thereby selected by choosing the variable moving

279 window with the lowest standard deviation (SD) of measured fluxes. This procedure was

280 repeated until the whole study period was parameterized.

281 Based on continuously monitored temperature and PAR (outside the chamber), R_{eco} , GPP and

282 NEE were modeled in half-hour steps for the entire study period. Because GPP was

283 parameterized based on PAR records inside but modeled with PAR records outside the chamber,

284 no PAR correction in terms of reduced light transmission was needed. Uncertainty of annual CO_2

285 exchange was quantified using a comprehensive error prediction algorithm described in detail by

286 Hoffmann et al. (2015).

287

288 **2.2.3 Modeling aboveground biomass dynamics**

289 Aboveground biomass development (NPP_{shoot}) was predicted using a logistic empirical model
290 (Yin et al., 2003; Zeide, 1993). From 2010 to 2012, modeled NPP_{shoot} was based on the
291 relationship between sampling date and the C content of harvested dry biomass measured during
292 sampling campaigns (three to four times per year following plant development). For alfalfa in
293 2013 and 2014, NPP_{shoot} was modeled based on biweekly measurements of LAI because no
294 additional biomass sampling was performed between the multiple cuts per year. To calculate the
295 C content corresponding to the measured LAI, the relationship between LAI prior to the chamber
296 harvest and the C content measured in the chamber harvest of all six alfalfa cuts was used. Daily
297 values of C stored within NPP_{shoot} were calculated using derived logistic functions.

298

299 **2.2.4 Calculation of ΔSOC**

300 Annual ΔSOC for each chamber was determined as the sum of annual NEE and NPP_{shoot} ,
301 representing C removal due to the chamber harvest (Eq. 4; Leifeld et al., 2014). Temporal
302 dynamics in ΔSOC were calculated as the sum of daily NEE and NPP_{shoot} .

303

$$304 \Delta SOC_n = \sum_{i=1}^n [NEE_i + CH_4 + (NPP_{shoot_i} - C_{import}) + \Delta DOC_i + \Delta DIC_i] \quad [Eq. 5]$$

305

306 Several minor components of Eq. 5 were not considered (see also Hernandez-Ramirez et al.,
307 2011). First, C import (C_{import}) due to seeding and fertilization, which was close to zero because
308 the measurement site was fertilized by a surface application of mineral fertilizer throughout the
309 entire study period. Second, methane (CH_4 -C) emissions, which were measured manually at the
310 same experimental field but did not exceed a relevant order of magnitude ($-0.01 \text{ g C m}^{-2} \text{ y}^{-1}$) and
311 were therefore not included in the ΔSOC calculation. Third, lateral C fluxes, originating from
312 dissolved organic (DOC) and inorganic carbon (DIC) as well as particulate soil organic carbon

313 (SOC_p). In addition to the rather small magnitude of the subsurface lateral C fluxes in soil
314 solution (Rieckh et al., 2012), it was assumed that their C input equaled C output at the plot scale.
315 Lateral SOC_p transport along the hillslope was excluded by grassland stripes established between
316 experimental plots in 2010 (Fig. 1 in Sommer et al., 2016).

317

318 **2.3 Soil resampling method**

319 To obtain ΔSOC using the soil resampling method, soil samples were collected three times
320 during the study period. Initial SOC along the topographic gradient was monitored prior to soil
321 manipulation during April 2009 at two soil pits, which were sampled by pedogenetic horizons.
322 After soil manipulation, a 5-m raster sampling of topsoils (Ap horizons) was performed during
323 April 2011. Each Ap horizon was separated into an upper (0-15 cm) and lower segment (15-25
324 cm), which were analyzed separately for bulk density, SOC, Nt and coarse fraction (< 2 mm)
325 (data not shown). From these data, SOC and Nt mass densities were calculated separately for
326 each segment and finally summed up for the entire Ap-horizon (0-25 cm). The mean SOC and Nt
327 content for the Ap horizon of each raster point was calculated by dividing SOC or Nt mass
328 densities (0-25 cm) through the fine-earth mass (0-25 cm). In December 2014, composite soil
329 samples of the Ap horizon were collected. The composite samples consist of samples from four
330 sampling points in a close proximity around each chamber. Prior to laboratory analysis coarse
331 organic material was discarded from collected soil samples (Schlichting et al. 1995).
332 Thermogravimetric desiccation at 105°C was performed in the laboratory for all samples to
333 determine bulk densities (Mg m⁻³). Bulk soil samples were air dried, gently crushed and sieved (2
334 mm) to obtain the fine fraction (particle size < 2 mm). The total carbon and total nitrogen
335 contents were determined by elementary analysis (TruSpec CNS analyzer, LECO Ltd.,
336 Mönchengladbach, Germany) as carbon dioxide via infrared detection after dry combustion at

337 1250°C (DIN ISO10694, 1996), in duplicate. As the soil horizons did not contain carbonates,
338 total carbon was equal to SOC.

339

340 **2.4 Uncertainty prediction and statistical analysis**

341 Uncertainty prediction for Δ SOC derived by the C budget method was performed according to
342 Hoffmann et al. (2015), following the law of error propagation. To test for differences in topsoil
343 SOC (SOC_{Ap}) and total nitrogen (Nt) stocks between soil resampling performed after soil
344 manipulation in 2010 and 2014, a paired *t*-test was applied. Computation of uncertainty
345 prediction and calculation of statistical analyses were performed using R 3.2.2.

346

347 **3. Results**

348 **3.1 C budget method**

349 **3.1.1 NEE and $\text{NPP}_{\text{shoot}}$ dynamics**

350 NEE and its components R_{eco} and GPP were characterized by a clear seasonality and diurnal
351 patterns. Seasonality followed plant growth and management events (e.g., harvest; Fig. 3),
352 Highest CO_2 uptake was thus observed during the growing season, whereas NEE fluxes during
353 the non-growing season were significantly lower. Diurnal patterns were more pronounced during
354 the growing season and less obvious during the non-growing season. In general R_{eco} fluxes were
355 higher during daytime, whereas GPP and NEE, in case of present cover crops, were lower or even
356 negative, representing a C uptake during daytime by the plant-soil system. Annual NEE was
357 crop dependent, ranging from $-1600 \text{ g C m}^{-2} \text{ y}^{-1}$ to $-288 \text{ g C m}^{-2} \text{ y}^{-1}$. Highest annual uptakes were
358 observed for maize and sorghum during 2011 and 2012, whereas alfalfa cultivation showed lower
359 annual NEE (Tab. 1). From 2010 to 2012, annual NEE followed the topographic gradient, with
360 higher NEE in the direction of the depression and lower NEE away from the depression. These

361 small-scale spatial differences in gaseous C exchange changed with alfalfa cultivation. As a
362 result, only minor differences between the chamber positions were observed, showing no clear
363 trend or tendency (Tab. 1).

364 C in living biomass (due to biomass sampling campaigns and LAI measurements) and C
365 removals due to harvest were in general well reflected by modeled NPP_{shoot} (Fig. 4). Annual C
366 removal due to harvest was clearly crop dependent, with highest NPP_{shoot} for maize and sorghum
367 ranging from 420 g C m^{-2} to 1238 g C m^{-2} , and lower values in the case of winter fodder rye and
368 alfalfa. Similar to NEE from 2010 to 2012, annual sums of NPP_{shoot} followed the topographic
369 gradient, with lower values close to the depression (Tab. 1). Again, lower differences in annual
370 NPP_{shoot} between the chambers and no spatial trends were found for alfalfa in 2013 and 2014.

371

372 **3.1.2 Δ SOC dynamics**

373 Temporal and spatial dynamics of continuously cumulated daily Δ SOC values during the four
374 years after soil manipulation are shown in Fig. 5. Differences in Δ SOC were in general less
375 pronounced during the non-growing season compared to the growing season. During the non-
376 growing season, differences were mainly driven by differences in R_{eco} rather than GPP or
377 NPP_{shoot} . This changed at the beginning of the growing season, when Δ SOC responded to
378 changes in cumulative NEE and NPP_{shoot} . Hence, up to 79 % of the standard deviation of
379 estimated annual Δ SOC developed during the period of maximum plant growth. Except for the
380 lower middle chamber position, alfalfa seemed to counterbalance spatial differences in Δ SOC
381 that developed during previous years (Fig. 5).

382 Annual Δ SOC values derived by the C budget method are presented in Tab. 1. Highest annual
383 SOC gains were obtained in 2012 for winter fodder rye and sorghum-Sudan grass, reaching an
384 average of $474 \text{ g C m}^{-2} \text{ y}^{-1}$. In contrast, maize cultivation during 2011 was characterized by C

385 losses between $59 \text{ g C m}^{-2} \text{ y}^{-1}$ and $169 \text{ g C m}^{-2} \text{ y}^{-1}$. However, prior to soil manipulation, maize
386 showed an average SOC gain of $102 \text{ g C m}^{-2} \text{ y}^{-1}$.

387

388 **3.2 Soil resampling method**

389 As a result of soil translocation in 2010, initially measured SOC_{Ap} stocks increased by an average
390 of 780 g C m^{-2} . However, due to the lower C content of the translocated topsoil material (0.76
391 %), the SOC_{Ap} content of the measurement site dropped by 10 - 14 % after soil manipulation
392 (Tab. 1). Significant differences (paired *t*-test; $t = -2.48$, $p < 0.09$), which showed an increase in
393 SOC_{Ap} of up to 11 %, were found between SOC_{Ap} stocks measured in 2010 and 2014. Three out
394 of the four chamber positions showed a C gain during the 4 measurement years following soil
395 manipulation. C gains were similar for the upper and lower chamber positions, but lower for the
396 upper middle position. No change in SOC was obtained in the case of the lower middle (Fig. 5;
397 Fig. 6) chamber position.

398

399 **3.3 Method comparison**

400 Average annual ΔSOC values for the soil resampling and C budget method are shown in Fig. 6.
401 ΔSOC based on these methods showed a good overall agreement, with similar tendencies and
402 magnitudes (Fig. 6). Irrespective of the applied method, significant differences were found
403 between SOC stocks measured directly after soil manipulation in 2010 and SOC stocks measured
404 in 2014. Following soil manipulation, both methods revealed similar tendencies in site and
405 chamber-specific ΔSOC (Fig. 6). Both methods indicated a clear C gain for three out of the four
406 chamber positions. C gains derived by the C budget method were similar for the upper, upper
407 middle and lower chamber positions. By contrast, C gains derived by the soil resampling method
408 were slightly but not significantly lower (paired *t*-test; $t = -1.23$, $p > 0.30$). This was most

409 pronounced for the upper middle chamber position. No change in Δ SOC and only a minor gain in
410 C was observed for the lower middle chamber position according to both methods. Differences
411 between chamber positions indicate the presence of small-scale spatial Δ SOC dynamics typical of
412 soils.

413

414 **4. Discussion**

415 **4.1 Accuracy and precision of applied methods**

416 Despite the similar magnitude and tendencies of the observed Δ SOC values, both methods were
417 subject to numerous sources of uncertainty. These errors affect the accuracy and precision of
418 observed Δ SOC values differently, which might help to explain differences between the soil
419 resampling and the C budget method.

420 The soil resampling method is characterized by high measurement precision, which allows for the
421 detection of relatively small changes in SOC. Related uncertainty in derived spatial and temporal
422 Δ SOC dynamics is therefore mainly attributed to the measurement accuracy, affected by
423 sampling strategy and design (Batjes and van Wesemael, 2015; De Gruijter et al., 2006). This
424 includes (i) the spatial distribution of collected samples, (ii) the sampling frequency, (iii) the
425 sampling depth and (iv) whether different components of soil organic matter (SOM) are excluded
426 prior to analyses. The first aspect determines the capability to detect the inherent spatial
427 differences in SOC stocks. This allows the conclusion that point measurements do not necessarily
428 represent AC measurements, which integrate over the spatial variability within their basal area.
429 The second aspect defines the temporal resolution, even though the soil resampling method is not
430 able to perfectly separate spatial from temporal variability because repeated soil samples are
431 biased by inherent spatial variability of the measurement site. The third aspect sets the vertical
432 system boundary, which is often limited because only topsoil horizons are sampled within a

433 number of soil monitoring networks (Van Wesemael et al., 2011) and repeated soil inventories
434 (Leifeld et al., 2011). Similarly, the fourth aspect defines which components of SOM are
435 specifically analyzed. Usually, coarse organic material is discarded prior to analysis (Schlichting
436 et al., 1995) and therefore, total SOC is not assessed (e.g., roots, harvest residues, etc.).

437 In comparison, the C budget method considers any type of organic material present in soil by
438 integrating over the total soil depth. As a result, both methods have a different validity range and
439 area, which makes direct quantitative comparison more difficult. This may explain the higher
440 uptake reported for three out of four chamber positions in the case of the C budget method.

441 In contrast to the soil resampling method, we postulate a higher accuracy and a lower precision in
442 the case of the AC-based C budget method. The reasons for this include a number of potential
443 errors affecting especially the measurement precision of the AC system, whereas over a constant
444 area and maximum soil depth, integrated AC measurements increase measurement accuracy.
445 First, it is currently not clear whether microclimatological and ecophysiological disturbances due
446 to chamber deployment, such as the alteration of temperature, humidity, pressure, radiation, and
447 gas concentration, may result in biased C flux rate estimates (Juszczak et al., 2013; Kutzbach et
448 al., 2007; Lai et al., 2012; Langensiepen et al., 2012). Second, uncertainties related to performed
449 flux separation and gap-filling procedures may influence the obtained annual gaseous C exchange
450 (Gomez-Casanovas et al., 2013; Görres et al., 2014; Moffat et al., 2007; Reichstein et al., 2005).

451 Although continuous operation of the AC system should allow for direct derivation of C budgets
452 from measured CO₂ exchange and annual yields, in practice, data gaps always occur. To fill the
453 measurement gaps, temperature- and PAR-dependent models are derived and used to calculate
454 R_{eco} and GPP, respectively (Hoffmann et al. 2015). Due to the transparent chambers used,
455 modeled R_{eco} is solely based on nighttime measurements. Hence, systematic differences between
456 nighttime and daytime R_{eco} will yield an over- or underestimation of modeled R_{eco}. Because

457 modeled R_{eco} is used to calculate GPP fluxes, GPP will be affected in a similar manner. However,
458 the systematic over- or underestimation of fluxes in both directions may counterbalance the
459 computed NEE, and estimated C budgets may be unaffected. Third, the development of $\text{NPP}_{\text{shoot}}$
460 underneath the chamber might be influenced by the permanently installed AC system. Fourth,
461 several minor components such as leaching losses of dissolved inorganic and organic carbon
462 (DIC and DOC), C transport via runoff and atmospheric C deposition were not considered within
463 the applied budgeting approach (see also 2.7).

464 Despite the uncertainties mentioned above, error estimates for annual NEE in this study are
465 within the range of errors presented for annual NEE estimates derived from EC measurements
466 (30 to $50 \text{ g C m}^{-2} \text{ y}^{-1}$) (e.g., Baldocchi, 2003; Dobermann et al., 2006; Hollinger et al., 2005) and
467 below the minimum detectable difference (MDD) reported for most repeated soil inventories
468 (e.g., Batjes and Van Wesemael, 2015; Knebl et al., 2015; Necpálová et al., 2014; Saby et al.,
469 2008; Schrumpf et al., 2011; VandenBygaart, 2006).

470

471 **4.2 Plausibility of observed ΔSOC**

472 Both the soil resampling and the C budget method showed C gains during the four years
473 following soil manipulation. A number of authors calculated additional C sequestration due to
474 soil erosion (Berhe et al., 2007; Dymond, 2010; VandenBygaart et al., 2015; Yoo et al., 2005),
475 which was explained by the burial of replaced C at depositional sites and dynamic replacement at
476 eroded sites (e.g., Doetterl et al., 2016). This is in accordance with erosion-induced C
477 sequestration postulated by, e.g., Berhe and Kleber (2013) and Van Oost et al. (2007). In
478 addition, observed C sequestration could also be a result of the manipulation-induced saturation
479 deficit in SOC. By adding topsoil material from an eroded unsaturated hillslope soil, the capacity
480 and efficiency to sequester C was theoretically increased (Stewart et al., 2007). Hence, additional

481 C was stored at the measurement site. This might be due to physicochemical processes, such as
482 physical protection in macro- and micro aggregates (Six et al., 2002) or chemical stabilization by
483 clay and iron minerals (Kleber et al., 2015).

484 Irrespective of the similar C gain observed by both methods, crop-dependent differences in
485 Δ SOC were only revealed by the C budget method. The reason is the higher temporal resolution
486 of AC-derived C budgets, displaying daily C losses and gains. Observed crop-dependent
487 differences in Δ SOC are in accordance with, e.g., Kutsch et al. (2010), Jans et al. (2010),
488 Hollinger et al. (2005) and Verma et al. (2005), who reported comparable EC-derived C balances
489 for inter alia, maize, sorghum and alfalfa.

490 In 2012, substantial positive annual Δ SOC values were observed. Due to low precipitation during
491 May and June, germination and plant growth of sorghum-Sudan grass was delayed (Fig. 4). As a
492 result, the reproductive phenological stage was drastically shortened. This reduced C losses prior
493 to harvest due to higher $R_{\text{eco}}:\text{GPP}$ ratios (Wagle et al., 2015). In addition, the presence of cover
494 crops during spring and autumn could have increased SOC, as reported by Lal et al. (2004),
495 Ghimire et al. (2014) and Sainju et al. (2002). No additional C sequestration was observed for
496 alfalfa in 2013 and 2014 or for the lower middle chamber position, which acted neither as a net C
497 source nor sink (Tab. 1; Fig. 5). This opposes the assumption of increased C sequestration by
498 perennial grasses (Paustian et al., 1997) or perennial crops (Zan et al., 2001). However, NEE
499 estimates of alfalfa were within the range of -100 to -400 g C m⁻², which is typical for forage
500 crops (*Lolium*, alfalfa, etc.) in different agro-ecosystems (Bolinder et al., 2012; Byrne et al.,
501 2005; Gilmanov et al., 2013; Zan et al., 2001). In addition, Alberti et al. (2010) reported a soil C
502 loss of > 170 g C m⁻² after crop conversion from continuous maize to alfalfa, concluding that no
503 effective C sequestration occurs in the short-term.

504 Regardless of the crop type, the AC-derived dynamic Δ SOC values showed that up to 79 % of
505 the standard deviation of estimated annual Δ SOC occurred during the growing season and the
506 main plant growth period from the beginning of July to the end of September.

507

508 **5. Conclusions**

509 We confirmed that AC-based C budgets are in principle able to detect small-scale spatial
510 differences and might be thus used to detect spatial heterogeneity of Δ SOC similar to the soil
511 resampling method. However, compared to soil resampling AC-based C budgets also reveal
512 short-term temporal dynamics. AC-derived C budgets showed not only pedon-scale differences
513 but also pronounced temporal dynamics in Δ SOC (Fig. 5). In addition, AC-based Δ SOC values
514 corresponded well with the tendencies and magnitude of the results observed in the repeated soil
515 inventory. The period of maximum plant growth was identified as being most important for the
516 development of spatial differences in annual Δ SOC. For upscaling purposes of the presented
517 results, further environmental drivers, processes and mechanisms determining C allocation in
518 space and time within the plant-soil system need to be identified. This type of an approach will be
519 pursued in future within the CarboZALF experimental setup (Sommer et al., 2016; Wehrhan et
520 al., 2016). Moreover, the AC-based C budget method opens new prospects for clarifying
521 unanswered questions, such as the influence of plant development or erosion on Δ SOC.

522

523 **Acknowledgments**

524 This work was supported by the Brandenburg Ministry of Infrastructure and Agriculture (MIL),
525 who financed the land purchase, the Federal Agency for Renewable Resources (FNR), who co-
526 financed the AC system, and the interdisciplinary research project CarboZALF. The authors want
527 to express their special thanks to Mr. Peter Rakowski for excellent operational and technical

528 maintenance during the study period as well as to the employees of the ZALF research station,
529 Dedelow, for establishing and maintaining the CarboZALF-D field trial.

530

531 **References**

- 532 Alberti, G., Delle Vedove, G.D., Zuliani, M., Peressotti, A., Castaldi, S., Zerbi, G., 2010.
533 Changes in CO₂ emissions after crop conversion from continuous maize to alfalfa. *Agric.*
534 *Ecosyst. Environ.* 136, 139-147.
- 535 Baldocchi, D.D., 2003. Assessing the eddy covariance technique for evaluating carbon dioxide
536 exchange rates of ecosystems: past, present and future. *Glob. Change Biol.* 9, 479-492.
- 537 Batjes, N.H., van Wesemael, B., 2015. Measuring and monitoring soil carbon, in: Banwart, S. A.,
538 Noellemeyer, E., Milne, E. (Eds.), *Soil Carbon: Science, Management and Policy for*
539 *Multiple Benefits*. SCOPE Series 71. CABI, Wallingford, UK, pp. 188-201.
- 540 Berhe, A.A., Harte, J., Harden, J.W., Torn, M.S., 2007. The significance of the erosion-induced
541 terrestrial carbon sink. *BioScience* 57, 337-346.
- 542 Berhe, A.A., Kleber, M., 2013. Erosion, deposition, and the persistence of soil organic matter:
543 mechanistic consideration and problems with terminology. *Earth Surf. Processes*
544 *Landforms* 38, 908-912.
- 545 Bolinder, M.A., Kätterer, T., Andrén, O., Parent, L.E., 2012. Estimating carbon inputs to soil in
546 forage-based crop rotations and modeling the effects on soil carbon dynamics in a
547 Swedish long-term field experiment. *Can. J. Soil. Sci.* 92, 821-833.
- 548 Byrne, K.A., Kiely, G., Leahy, P., 2005. CO₂ fluxes in adjacent new and permanent temperate
549 grasslands. *Agric. For. Meteorol.* 135, 82-92.

550 Chen, L., Smith, P., Yang, Y., 2015. How has soil carbon stock changed over recent decades?
551 Glob. Change Biol. 21, 3197-3199.

552 Conant, R.T., Ogle, S.M., Paul, E.A., Paustian, K., 2011. Measuring and monitoring soil organic
553 carbon stocks in agricultural lands for climate mitigation. Front. Ecol. Environ. 9, 169-
554 173.

555 Culman, S.W., Snapp, S.S., Green, J.M., Gentry, L.E., 2013. Short- and long-term labile soil
556 carbon and nitrogen dynamics reflect management and predict corn agronomic
557 performance. Agron. J. 105, 493-502.

558 Davidson, E. A., Savage, K., Verchot, L. V., Navarro, R., 2002. Minimizing artifacts and biases
559 in chamber-based measurements of soil respiration. Agric. For. Meteorol. 113, 21-37.

560 De Gruijter, J.J., Brus, D.J., Bierkens, M.F.P., Knotters, M., 2006. Sampling for Natural
561 Resource Monitoring. Springer Verlag, Berlin.

562 Dobermann, A.R., Walters, D.T., Baker, J.M., 2006. Comment on “Carbon budget of mature no-
563 till ecosystem in north central region of the United States.” Agric. For. Meteorol. 136, 83-
564 84.

565 Doetterl, S., Berhe, A.A., Nadeu, E., Wang, Z., Sommer, M., Fiener, P., 2016. Erosion,
566 deposition and soil carbon: a review of process-level controls, experimental tools and
567 models to address C cycling in dynamic landscapes. Earth Sci. Rev. 154, 102-122.

568 Dymond, J.R., 2010. Soil erosion in New Zealand is a net sink of CO₂. Earth Surf. Processes
569 Landforms 35, 1763-1772. doi:10.1002/esp.2014.

570 Eickenscheidt, T., Freibauer, A., Heinichen, J., Augustin, J., Drösler, M., 2014. Short-term
571 effects of biogas digestate and cattle slurry application on greenhouse gas emissions
572 affected by N availability from grasslands on drained fen peatlands and associated organic
573 soils. Biogeosciences 11, 6187-6207.

574 Elsgaard, L., Görres, C., Hoffmann, C.C., Blicher-Mathiesen, G., Schelde, K., Petersen, S.O.,
575 2012. Net ecosystem exchange of CO₂ and carbon balance for eight temperate organic
576 soils under agricultural management. *Agric. Ecosyst. Environ.* 162, 52-67.

577 Foken, T., 2008. *Micrometeorology*. Springer Verlag, Berlin.

578 Ghimire, R., Norton, J.B., Pendall, E., 2014. Alfalfa-grass biomass, soil organic carbon, and total
579 nitrogen under different management approaches in an irrigated agroecosystem. *Plant Soil*
580 374, 173-184.

581 Gilmanov, T.G., Soussana, J.F., Aires, L., Allard, V., Ammann, C., Balzarolo, M., Barcza, Z.,
582 Bernhofer, C., Campbell, C.L., Cernusca, A., Cescatti, A., Clifton-Brown, J., Dirks,
583 B.O.M., Dore, S., Eugster, W., Fuhrer, J., Gimeno, C., Gruenwald, T., Haszpra, L.,
584 Hensen, A., Ibrom, A., Jacobs, A.F.G., Jones, M.B., Lanigan, G., Laurila, T., Lohila, A.,
585 Manca, G., Marcolla, B., Nagy, Z., Pilegaard, K., Pinter, K., Pio, C., Raschi, A., Rogiers,
586 N., Sanz, M.J., Stefani, P., Sutton, M., Tuba, Z., Valentini, R., Williams, M.L., Wohlfahrt,
587 G., 2007. Partitioning European grassland net ecosystem CO₂ exchange into gross
588 primary productivity and ecosystem respiration using light response function analysis.
589 *Agric. Ecosyst. Environ.* 121, 93–120.

590 Gilmanov, T.G., Wylie, B.K., Tieszen, L.L., Meyers, T.P., Baron, V.S., Bernacchi, C.J.,
591 Billesbach, D.P., Burba, G.G., Fischer, M.L., Glenn, A.J., Hanan, N.P., Hatfield, J.L.,
592 Heuer, M.W., Hollinger, S.E., Howard, D.M., Matamala, R., Prueger, J.H., Tenuta, M.,
593 Young, D.G., 2013. CO₂ uptake and ecophysiological parameters of the grain crops of
594 midcontinent North America: estimates from flux tower measurements. *Agric. Ecosyst.*
595 *Environ.* 164, 162–175.

596 Gomez-Casanovas, N., Anderson-Teixeira, K., Zeri, M., Bernacchi, C.J., DeLucia, E.H., 2013.
597 Gap filling strategies and error in estimating annual soil respiration. *Glob. Change Biol.*
598 19, 1941-1952.

599 Görres, C.-M., Kutzbach, L., Elsgaard, L., 2014. Comparative modeling of annual CO₂ flux of
600 temperate peat soils under permanent grassland management. *Agric. Ecosyst. Environ.*
601 186, 64–76.

602 Hernandez-Ramirez, G., Hatfield, J.L., Parkin, T.B., Sauer, T.J., Prueger, J.H., 2011. Carbon
603 dioxide fluxes in corn-soybean rotation in the midwestern U.S.: inter- and intra-annual
604 variations, and biophysical controls. *Agric. For. Meteorol.* 151, 1831-1842.

605 Hoffmann, M., Jurisch, N., Borraz, E.A., Hagemann, U., Drösler, M., Sommer, M., Augustin, J.,
606 2015. Automated modeling of ecosystem CO₂ fluxes based on periodic closed chamber
607 measurements: a standardized conceptual and practical approach. *Agric. For. Meteorol.*
608 200, 30-45.

609 Hollinger, S.E., Bernacchi, C.J., Meyers, T.P., 2005. Carbon budget of mature no-till ecosystem
610 in north central region of the United States. *Agric. For. Meteorol.* 130, 59-69.

611 IUSS Working Group WRB, 2015. World reference base for soil resources 2014. International
612 soil classification system for naming soils and creating legends for soil maps. Update
613 2015. World Soil Resources Reports No. 106. FAO, Rome.

614 Jans, W.W.P., Jacobs, C.M.J., Kruijt, B., Elbers, J.A., Barendse, S., Moors, E.J., 2010. Carbon
615 exchange of a maize (*Zea mays* L.) crop: influence of phenology. *Agric. Ecosyst.*
616 *Environ.* 139, 316-324.

617 Juszczak, R., Humphreys, E., Acosta, M., Michalak-Galczewska, M., Kayzer, D., Olejnik, J.,
618 2013. Ecosystem respiration in a heterogeneous temperate peatland and its sensitivity to
619 peat temperature and water table depth. *Plant Soil* 366, 505-520.

620 Kleber, M., Eusterhues, K., Keiluweit, M., Mikutta, C., Mikutta, R., Nico, P. S., 2015. Chapter
621 one – Mineral-Organic associations: Formation, Properties, and relevance in soil
622 environments. *Adv. Agro.* 130, 1-140.

623 Knebl, L., Leithold, G., Brock, C., 2015. Improving minimum detectable differences in the
624 assessment of soil organic matter change in short-term field experiments. *J. Plant Nutr.*
625 *Soil Sci.* 178, 35-42.

626 Koskinen, M., Minkkinen, K., Ojanen, P., Kämäräinen, M., Laurila, T., Lohila, A., 2014.
627 Measurements of CO₂ exchange with an automated chamber system throughout the year:
628 challenges in measuring night-time respiration on porous peat soil. *Biogeosciences* 11,
629 347-363.

630 Kutsch, W.L., Aubinet, M., Buchmann, N., Smith, P., Osborne, B., Eugster, W., Wattenbach, M.,
631 Schruppf, M., Schulze, E.D., Tomelleri, E., Ceschia, E., Bernhofer, C., Béziat, P.,
632 Carrara, A., Di Tommasi, P., Grünwald, T., Jones, M., Magliulo, V., Marloie, O.,
633 Moureaux, C., Olioso, A., Sanz, M.J., Saunders, M., Søgaard, H., Ziegler, W., 2010. The
634 net biome production of full crop rotations in Europe. *Agric. Ecosyst. Environ.* 139, 336-
635 345.

636 Kutzbach, L., Schneider, J., Sachs, T., Giebels, M., Nykänen, H., Shurpali, N.J., Martikainen,
637 P.J., Alm, J., Wilmking, M., 2007. CO₂ flux determination by closed-chamber methods
638 can be seriously biased by inappropriate application of linear regression. *Biogeosciences*
639 4, 1005-1025.

640 Lai, D.Y.F., Roulet, N.T., Humphreys, E.R., Moore, T.R., Dalva, M., 2012. The effect of
641 atmospheric turbulence and chamber deployment period on autochamber CO₂ and CH₄
642 flux measurements in an ombrotrophic peatland. *Biogeosciences* 9, 3305-3322.

643 Lal, R., Griffin, M., Apt, J., Lave, L., Morgan, G., M., 2004. Managing Soil carbon. *Science* 304,
644 393.

645 Langensiepen, M., Kupisch, M., van Wijk, M.T., Ewert, F., 2012. Analyzing transient closed
646 chamber effects on canopy gas exchange for flux calculation timing. *Agric. For.*
647 *Meteorol.* 164, 61-70.

648 Leiber-Sauheitl, K., Fuß, R., Voigt, C., Freibauer, A., 2013. High greenhouse gas fluxes from
649 grassland on histic gleysol along soil C and drainage grasslands. *Biogeosci. Discuss.* 10,
650 11283-11317.

651 Leifeld, J., Ammann, C., Neftel, A., Fuhrer, J., 2011. A comparison of repeated soil inventory
652 and carbon flux budget to detect soil carbon stock changes after conversion from cropland
653 to grasslands. *Glob. Change Biol.* 17, 3366-3375.

654 Leifeld, J., Bader, C., Borraz, E., Hoffmann, M., Giebels, M., Sommer, M., Augustin, J., 2014.
655 Are C-loss rates from drained peatlands constant over time? The additive value of soil
656 profile based and flux budget approach. *Biogeosci. Discuss.* 11, 12341-12373.

657 Livingston, G.P., Hutchinson, G.L., 1995. Enclosure-based measurement of trace gas exchange:
658 applications and sources of error, in: Matson, P.A., Harris, R.C. (Eds.), *Methods in*
659 *Ecology. Biogenic Trace Gases: Measuring Emissions from Soil and Water.* Blackwell
660 Science, Oxford, UK, pp. 14–51.

661 Lloyd, J., Taylor, J.A., 1994. On the temperature dependence of soil respiration. *Funct. Ecol.* 8,
662 315-323.

663 Luo, Y., Ahlström, A., Allison, S.D., Batjes, N.H., Brovkin, V., Carvalhais, N., Chappell, A.,
664 Ciais, P., Davidson, E.A., Finzi, A., Georgiou, K., Guenet, B., Hararuk, O., Harden, J.W.,
665 He, Y., Hopkins, F., Jiang, L., Koven, C., Jackson, R.B., Jones, C.D., Lara, M.J., Liang,
666 J., McGuire, A.D., Parton, W., Peng, C., Randerson, J.T., Salazar, A., Sierra, C.A., Smith,

667 M.J., Tian, H., Todd-Brown, K.E.O., Torn, M., van Groenigen, k.J., Wang, Y.P., West,
668 t.o., Wie, Y., Wieder, W.R., Xia, J., Xu, X., Xu, X., Zhou, T., 2016. Toward more
669 realistic projections of soil carbon dynamics by Earth system models. *Global*
670 *Biogeochem. Cycles* 30, 40-56.

671 Moffat, A.M., Papale D., Reichstein M., Hollinger, D.Y., Richardson, A.D., Barr, A.G.,
672 Beckstein, C., Braswell, B.H., Churkina, G., Desai, A.R., Falge, E., Gove, J.H., Heimann,
673 M., Hui, D., Jarvis, A.J., Kattge, J., Noormets, A., Stauch, V.J., 2007. Comprehensive
674 comparison of gap-filling techniques for eddy covariance net carbon fluxes. *Agric. For.*
675 *Meteorol.* 147, 209–232.

676 Necpálová, M., Anex Jr., R.P., Kravchenko, A.N., Abendroth, L.J., Del Grosso, S.J., Dick, W.A.,
677 Helmers, M.J., Herzmann, D., Lauer, J.G., Nafziger, E.D., Sawyer, J.E., Scharf, P.C.,
678 Strock, J.S., Villamil, M.B., 2014. What does it take to detect a change in soil carbon
679 stock? A regional comparison of minimum detectable difference and experiment duration
680 in the north central United States. *J. Soils Water Conserv.* 69, 517-531.

681 Paustian, K., Collins, H.P., Paul, E.A., 1997. Management controls on soil carbon, in: Paul, E.A.,
682 Paustian, K., Elliott, E.T., Cole, C.V. (Eds.), *Soil Organic Matter in Temperate*
683 *Agroecosystems: Long-Term Experiments in North America*. CRC Press, Boca Raton,
684 FL, pp. 15-50.

685 Poeplau, C., Bolinder, M.A., Kätterer, T., 2016. Towards an unbiased method for quantifying
686 treatment effects on soil carbon in long-term experiments considering initial within-field
687 variation. *Geoderma* 267, 41-47.

688 Pohl, M., Hoffmann, M., Hagemann, U., Giebels, M., Albiac Borraz, E., Sommer, M., Augustin,
689 J., 2014. Dynamic C and N stocks—key factors controlling the C gas exchange of maize in
690 a heterogeneous peatland. *Biogeosciences* 11, 2737-2752.

691 Reichstein, M., Falge, E., Baldocchi, D., Papale, D., Aubinet, M., Berbigier, P., Bernhofer, C.,
692 Buchmann, N., Gilmanov, T., Granier, A., Grünwald, T., Havránková, K., Ilvesniemi, H.,
693 Janous, D., Knohl, A., Laurila, T., Lohila, A., Loustau, D., Metteucci, G., Meyers, T.,
694 Miglietta, F., Ourcival, J.-M., Pumpanen, J., Rambal, S., Rotenberg, E., Sanz, M.,
695 Tenhunen, J., Seufert, G., Vaccari, F., Vesala, T., Yakir, D., Valentini, R., 2005. On the
696 separation of net ecosystem exchange into assimilation and ecosystem respiration: review
697 and improved algorithm. *Global Change Biol.* 11, 1424–1439.

698 Rieckh, H., Gerke, H.H., Sommer, M., 2012. Hydraulic properties of characteristic horizons
699 depending on relief position and structure in a hummocky glacial soil landscape. *Soil*
700 *Tillage Res.* 125, 123-131.

701 Saby, N.P.A., Bellamy, P.H., Morvan, X., Arrouays, D., Jones, R.J.A., Verheijen, F.G.A.,
702 Kibblewhite, M.G., Verdoodt, A., Üveges, J.B., Freudenschuß, A., Simota, C., 2008. Will
703 European soil-monitoring networks be able to detect changes in topsoil organic carbon
704 content? *Glob. Change Biol.* 14, 2432-2442.

705 Sainju, U.M., Singh, B.P., Whitehead, W.F., 2002. Long-term effects of tillage, cover crops, and
706 nitrogen fertilization on organic carbon and nitrogen concentrations in sandy loam soils in
707 Georgia, USA. *Soil Tillage Res.* 63, 167-179.

708 Savage, K.E., Davidson, E.A., 2003. A comparison of manual and automated systems for soil
709 CO₂ flux measurements: trade-offs between spatial and temporal resolution. *J. Exp. Bot.*
710 54, 891-899.

711 Schlichting, E., Blume, H.P., Stahr, K., *Soils Practical* (in German). Blackwell, Berlin, 1995.

712 Schrumpf, M., Schulze, E. D., Kaiser, K., Schumacher, J., 2011. How accurately can soil organic
713 carbon stocks and stock changes be quantified by soil inventories? *Biogeosciences* 8,
714 1193-1212.

715 Six, J., Conant, R.T., Paul, E.A., Paustian, K., 2002. Stabilization mechanisms of soil organic
716 matter: implications for C-saturation of soils. *Plant Soil* 241, 155-176.

717 Skinner, R.H., Dell, C.J., 2015. Comparing pasture C sequestration estimates from eddy
718 covariance and soil cores. *Agric. Ecosyst. Environ.* 199, 52-57.

719 Smith, P., Lanigan, G., Kutsch, W. L., Buchmann, N., Eugster, W., Aubinet, M., Ceschia, E.,
720 Béziat, P., Yeluripati, J. B., Osborne, B., Moors, E. J., Brut, A., Wattenbach, M.,
721 Saunders, M., Jones, M., 2010. Measurements necessary for assessing the net ecosystem
722 carbon budget of croplands. *Agric. Ecosyst. Environ.* 139, 302-315.

723 Sommer, M., Augustin, J., Kleber, M., 2016. Feedbacks of soil erosion on SOC patterns and
724 carbon dynamics in agricultural landscapes – the CarboZALF experiment. *Soil Tillage
725 Res.* 156, 182-184.

726 Stewart, C.E., Paustian, K., Conant, R.T., Plante, A.F., Six, J., 2007. Soil carbon saturation:
727 concept, evidence and evaluation. *Biogeochemistry* 86, 19-31.

728 Stockmann, U., Padarian, J., McBratney, A., Minasny, B., de Brogniez, D., Montanarella, L.,
729 Hong, Y., S., Rawlins, B.G., Field, D.J., 2015. Global soil organic carbon assessment.
730 *Glob. Food Secur.* 6, 9-16.

731 Van Oost, K., Quine, T.A., Govers, G., De Gryze, S., Six, J., Harden, J.W., Ritchie, J.C.,
732 McCarty, G.W., Heckrath, G., Kosmas, C., Giraldez, J.V., da Silva, J.R., Merckx, R.,
733 2007. The impact of agricultural soil erosion on the global carbon cycle. *Science* 318,
734 626-629.

735 Van Wesemael, B., Paustian, K., Andrén, O., Cerri, C.E.P., Dodd, M., Etchevers, J., Goidts, E.,
736 Grace, P., Kätterer, T., McConkey, B.G., Ogle, S., Pan, G., Siebner, C., 2011. How can
737 soil monitoring networks be used to improve predictions of organic carbon pool dynamics
738 and CO₂ fluxes in agricultural soils? *Plant Soil* 338, 247-259.

739 VandenBygaart, A.J., 2006. Monitoring soil organic carbon stock changes in agricultural
740 landscapes: issues and a proposed approach. *Can. J. Soil Sci.* 86, 451-463.

741 VandenBygaart, A.J., Gregorich, E.G., Helgason, B.L., 2015. Cropland C erosion and burial: is
742 buried soil organic matter biodegradable? *Geoderma* 239-240, 240-249.

743 Verma, S.B., Dobermann, A., Cassman, K.G., Walters, D.T., Knops, J.M., Arkebauer, T.J.,
744 Suyker, A.E., Burba, G.G., Amos, B., Yang, H., Ginting, D., Hubbard, K.G., Gitelson,
745 A.A., Walter-Shea, E.A., 2005. Annual carbon dioxide exchange in irrigated and rainfed
746 maize-based agroecosystems. *Agric. For. Meteorol.* 131, 77-96.

747 Wagle, P., Kakani, V.G., Huhnke, R.L., 2015. Net ecosystem carbon dioxide exchange of
748 dedicated bioenergy feedstocks: switchgrass and high biomass sorghum. *Agric. For.*
749 *Meteorol.* 207, 107-116.

750 Wang, K., Liu, C., Zheng, X., Pihlatie, M., Li, B., Haapanala, S., Vesala, T., Liu, H., Wang, Y.,
751 Liu, G., Hu, F., 2013. Comparison between eddy covariance and automatic chamber
752 techniques for measuring net ecosystem exchange of carbon dioxide in cotton and wheat
753 fields. *Biogeosciences* 10, 6865-6877.

754 Wehrhan, M., Rauneker, P., Sommer, M., 2016. UAV-based estimation of carbon exports from
755 heterogeneous soil landscapes - a case study from the CarboZALF experimental area.
756 *Sensors (Basel)* 16, 255.

757 Wuest, S., 2014. Seasonal variation in soil organic carbon. *Soil Sci. Soc. Am. J.* 78, 1442-1447.

758 Xiong, X., Grunwald, S., Corstanje, R., Yu, C., Bliznyuk, N., 2016. Scale-dependent variability
759 of soil organic carbon coupled to land use and land cover. *Soil Tillage Res.* 160, 101-109.

760 Yin, X., Goudriaan, J., Lantinga, E.A., Vos, J., Spiertz, H.J., 2003. A flexible sigmoid function of
761 determinate growth. *Ann. Bot.* 91, 361-371.

762 Yoo, K., Amundson, R., Heimsath, A.M., Dietrich, W.E., 2005. Erosion of upland hillslope soil
763 organic carbon: coupling field measurements with a sediment transport model. *Global*
764 *Biogeochem. Cycles* 19, 1-17.

765 Zan, C.S., Fyles, J.W., Girouard, P., Samson, R.A., 2001. Carbon sequestration in perennial
766 bioenergy, annual corn and uncultivated systems in southern Quebec. *Agric. Ecosyst.*
767 *Environ.* 86, 135-144.

768 Zeide, B., 1993. Analysis of growth equations. *For. Sci.* 39, 594-616.

769

770 **List of tables:**

771 **Tab. 1.:** Chamber-specific annual sums of CO₂ exchange (R_{eco}, GPP, NEE), NPP_{shoot} and ΔSOC
772 (± uncertainty), as well as corresponding environmental variables measured during the study
773 period from 2010 to 2014.

774 **A.1.:** Management information regarding the study period from 2010 to 2014. Gray shaded rows
775 indicate coverage by chamber measurements.

776

777 **List of figures:**

778 **Fig. 1.:** Schematic representation of the study concept. Black stars represent SOC measured by
779 the soil resampling method. Black circles represent annual SOC derived using the C budget
780 method.

781 **Fig. 2.:** Transect of automatic chambers and chamber positions within the depression overlying
782 the Endogleyic Colluvic Regosol (WRB 2015, left). The black arrow shows the position of the
783 datalogger and controlling devices, which were placed within a wooden, weather-sheltered house.

784 The soil profile is shown on the right. Soil horizon-specific SOC (%) and Nt (%) contents are
785 indicated by solid and dashed vertical white lines, respectively. Spatial differences in Δ SOC and
786 the basic principle of the C budget method are shown as the scheme within the picture.

787 **Fig. 3.:** Time series of CO₂ exchange (A-D) for the four chambers of the AC system during the
788 study period from 2010 to 2014. R_{eco} (black), GPP (light gray) and NEE (dark gray) are shown as
789 daily sums (y-axis). NEE_{cum} is presented as a solid line, representing the sum of continuously
790 accumulated daily NEE values (secondary y-axis). The presented values display cumulative NEE
791 following soil manipulation to the end of 2014. Note the different scales of the y-axes. The grey
792 shaded area represents the period prior to soil manipulation. The dashed vertical line indicates the
793 soil manipulation. Dotted lines represent harvest events.

794 **Fig. 4.:** Time series of modeled aboveground biomass development (NPP_{shoot}) (A-D) for the four
795 chambers of the AC system during the study period from 2010 to 2014. NPP_{shoot} is shown as
796 cumulative values. The presented values display cumulative NPP_{shoot} following soil manipulation
797 to the end of 2014. The biomass model is based on biomass sampling (2010-2012) and biweekly
798 LAI measurements (2013-2014) during crop growth (grey dots). C removal due to chamber
799 harvests is shown by black dots. The grey shaded area represents the period prior to soil
800 manipulation. The dashed vertical line indicates the soil manipulation. Dotted lines represent
801 harvest events.

802 **Fig. 5.:** Temporal and spatial dynamics in cumulative Δ SOC throughout the study period based
803 on (A) the C budget method (measured/modeled; black lines) and (B) the soil resampling method
804 (linear interpolation; gray lines). The grey shaded area represents the period prior to soil
805 manipulation. The dashed vertical line indicates the soil manipulation. Dotted lines represent
806 harvest events. Temporal dynamics revealed by the C budget method allow for the identification

807 of periods being most important for the development of Δ SOC. Major spatial deviation occurred
808 during the maximum plant growth period (May to September). The proportion (%) of these
809 periods with respect to the standard deviation of estimated annual Δ SOC accounted for up to 79
810 %.

811 **Fig. 6.:** Average annual Δ SOC observed after soil manipulation (April 2011 to December 2014)
812 by soil resampling and the C budget method for (A) the entire measurement site and (B) single
813 chamber positions within the measured transect. Δ SOC represents the change in carbon storage,
814 with positive values indicating C sequestration and negative values indicating C losses. Error bars
815 display estimated uncertainty for the C budget method and the analytical error of $\pm 5\%$ for the
816 soil resampling method. A performed Wilcoxon rank-sum test showed no significant difference
817 between Δ SOC values obtained by both methodological approaches for all four chambers (p-
818 value=0.25).

819 **A.3.:** Time series of recorded environmental conditions throughout the study period from 2010 to
820 2014. Daily Precipitation and GWL are shown for the upper (solid line) and lower (dashed line)
821 chamber position in the upper panel (A). The lower panel (B) shows the mean daily air
822 temperature. The grey shaded area represents the period prior to soil manipulation. The dashed
823 vertical line indicates the soil manipulation.

824

825

826

827

828

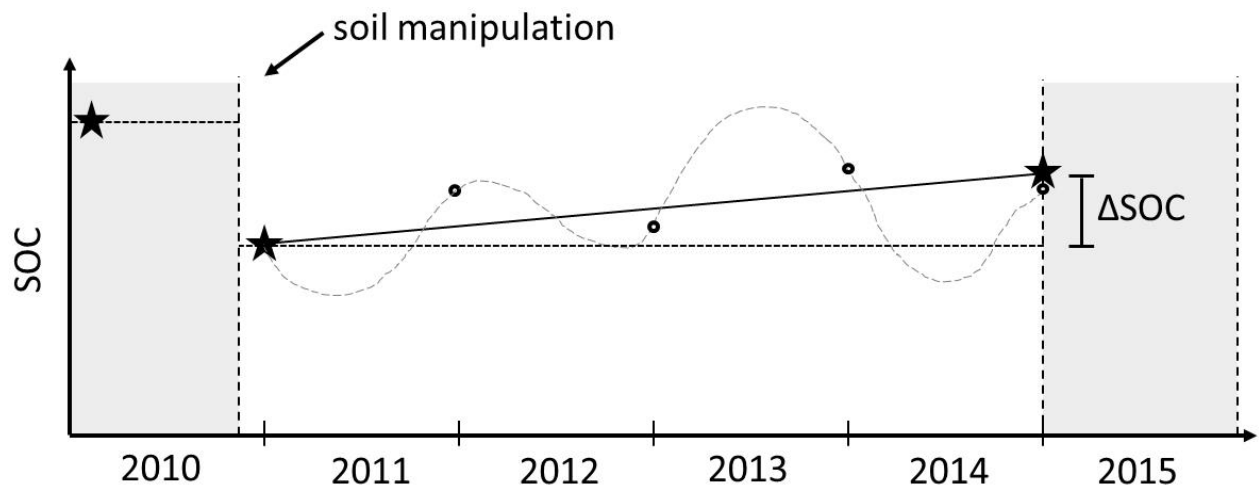
Tab.1

Year	Crop rotation	Position	R _{co2}	GPP	NEE	ASOC (C budget)	NPP _{shoot}			SOC to 1 m depth	SOC in Ap horizon	ΔSOC (soil inventory)	Nt to 1 m depth	Nt in Ap horizon	Precip.	GWL		
							harvested	modeled	N								P	K
							(g C m ⁻²)	(g C m ⁻²)	(g m ⁻²)								(Kg m ⁻² 1 m ⁻¹)	(Kg m ⁻² 0.3 m ⁻¹)
2010	maize	A (upper)	1014 ±9	-1845 ±8	-831 ^a ±12	86 ±66	744	745 ^a ±65	28.1	5.0	25.6	11.6	5.1		1.3	0.6	516	135
		B (upper middle)	987 ±11	-1970 ^a ±8	-983 ±13	251 ±66	727	732 ^a ±64	24.7	4.1	18.0	9.1	4.2		0.9	0.4		103
		C (lower middle)	1064 ±38	-2000 ^a ±11	-935 ^a ±40	190 ±77	744	745 ^a ±65	25.5	4.2	16.9	9.1	4.2		0.9	0.4		95
		D (lower)	1110 ±21	-1737 ±10	-627 ^a ±23	-118 ±69	744	745 ^a ±65	25.0	4.2	18.2	12.8	5.0		1.3	0.5		69
2011	maize	A (upper)	891 ±13	-2022 ±18	-1131 ^a ±22	-149 ±103	1238	1280 ^a ±101	29.5	5.4	30.2	10.5	3.5		1.1	0.4	618	129
		B (upper middle)	855 ^a ±10	-1894 ±13	-1039 ^a ±16	-169 ±96	1167	1208 ^a ±95	36.4	5.9	32.7	8.7	3.4		0.9	0.4		97
		C (lower middle)	980 ±14	-2062 ±25	-1082 ±28	-79 ±95	1115	1161 ^a ±91	33.7	5.6	32.9	9.0	3.7		0.9	0.4		87
		D (lower)	843 ^a ±31	-1730 ±8	-888 ±32	-59 ±80	900	947 ^a ±73	35.0	5.7	31.8	12.2	4.0		1.3	0.4		61
2012	winter wheat	A (upper)	1058 ±86	-2659 ±12	-1600 ±87	648 ±104	297 ^a /634	952 ^a ±56	36.3	6.3	42.6						585	139
		B (upper middle)	1075 ±8	-2591 ±11	-1516 ±13	472 ±65	310 ^a /727	1044 ^a ±64	33.3	5.8	37.5							107
2012	sorghum	C (lower middle)	1286 ±8	-2617 ±9	-1331 ±12	346 ±60	310 ^a /665	985 ^a ±59	32.7	5.4	35.5							87
		D (lower)	1044 ±10	-2194 ±9	-1150 ±13	430 ±39	299 ^a /420	720 ^a ±37	33.9	5.8	40.4							61
2013	alfalfa	A (upper)	1140 ±83	-1583 ±9	-443 ±83	43 ±91	290	400 ^b ±37	14.0	1.7	11.6						499	154
		B (upper middle)	1283 ±80	-1819 ±8	-536 ±80	93 ±86	304	443 ^b ±32	14.7	1.8	12.1							122
		C (lower middle)	1438 ±20	-1726 ±7	-288 ±22	-107 ±36	324	395 ^a ±29	15.6	1.9	12.9							94
		D (lower)	1587 ±80	-2036 ±8	-448 ±80	6 ±87	329	442 ^b ±34	15.9	2.0	13.2							68
2014	alfalfa	A (upper)	1161 ±15	-1615 ±7	-455 ^a ±16	-126 ±26	605	581 ^a ±20	29.2	3.6	24.2	10.9	3.9	376	1.2	0.5	591	181
		B (upper middle)	1443 ±18	-2063 ±7	-619 ^a ±19	52 ±28	635	567 ^a ±20	30.7	3.8	25.4	8.9	3.5	156	0.9	0.4		149
		C (lower middle)	1683 ±18	-2111 ±6	-428 ±19	-36 ±26	632	535 ^a ±18	30.5	3.8	25.3	9.0	3.7	0	0.9	0.5		121
		D (lower)	1584 ±12	-2113 ±14	-528 ±19	-52 ±28	587	580 ^a ±21	28.3	3.5	23.5	12.5	4.2	276	1.3	0.4		95
annual average (2011-2014)	site	A (upper)	1063 ±49	-1970 ±12	-901 ±52	98 ±43	766	803 ±54	27.3	4.3	27.2			94 ±43				151
		B (upper middle)	1164 ±29	-2092 ±10	-919 ±32	104 ±37	786	815 ±53	28.8	4.3	26.9			39 ±43				119
		C (lower middle)	1347 ±15	-2129 ±12	-779 ±20	10 ±30	762	769 ±49	28.1	4.2	26.7			0 ±46			573	97
		D (lower)	1265 ±33	-2018 ±10	-739 ±38	67 ±32	634	672 ±41	28.3	4.3	27.2			69 ±47				71
		site	1209 ±32	-2052 ±11	-843 ±36	78 ±18	737	765 ±49	28.1	4.3	27.0			51 ±18				156

* NPP_{shoot} is based on biomass samples collected next to each chamber because no chamber harvest was performed for *winter fodder rye* in 2012; superscript letter indicate non-significant differences

(Wilcoxon rank sum test; p-value > 0.05) between measured CO₂ fluxes and NPP_{shoot}.

832 Fig. 1



833

834

835

836

837

838

839

840

841

842

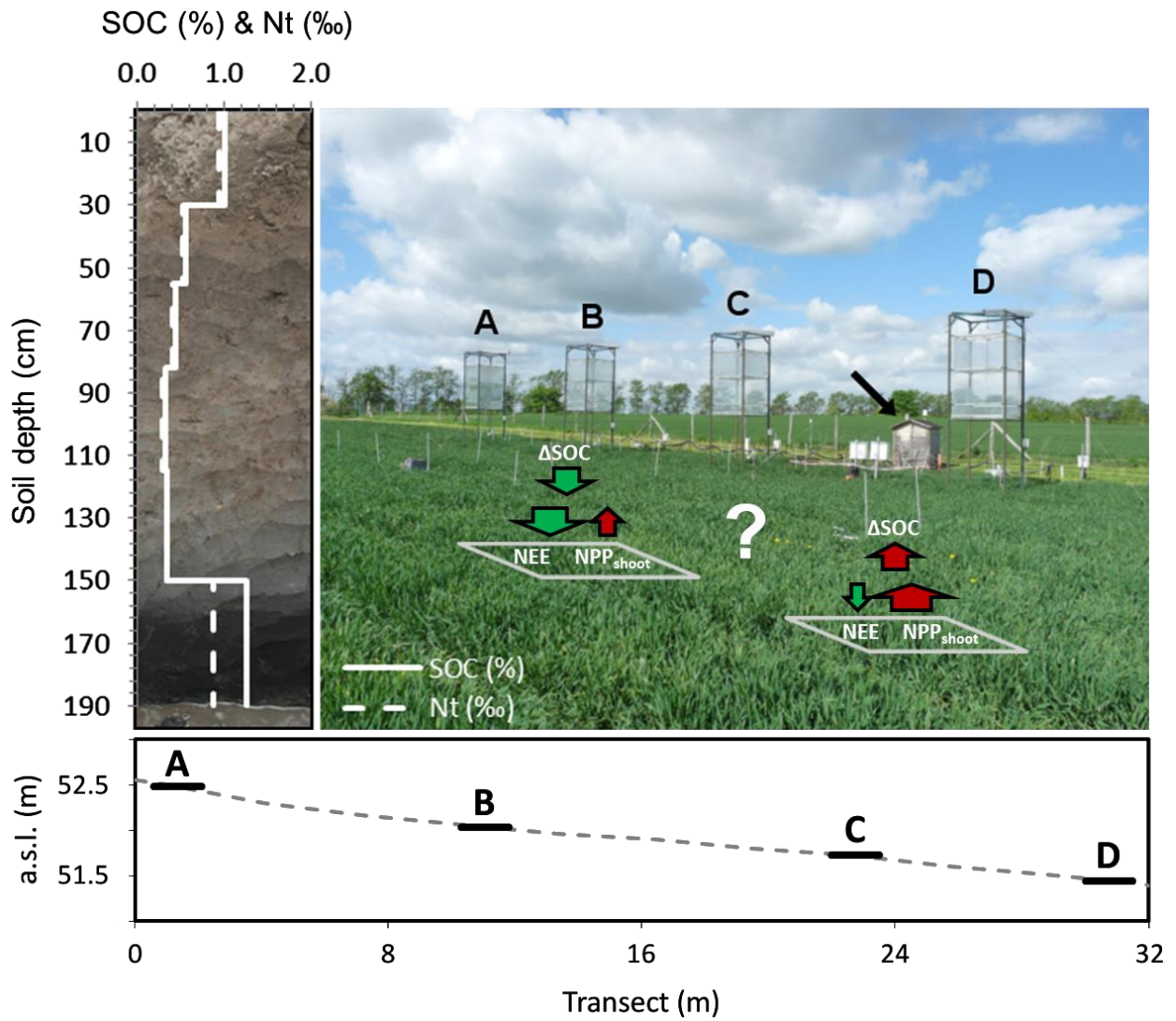
843

844

845

846

847 **Fig. 2**



848

849

850

851

852

853

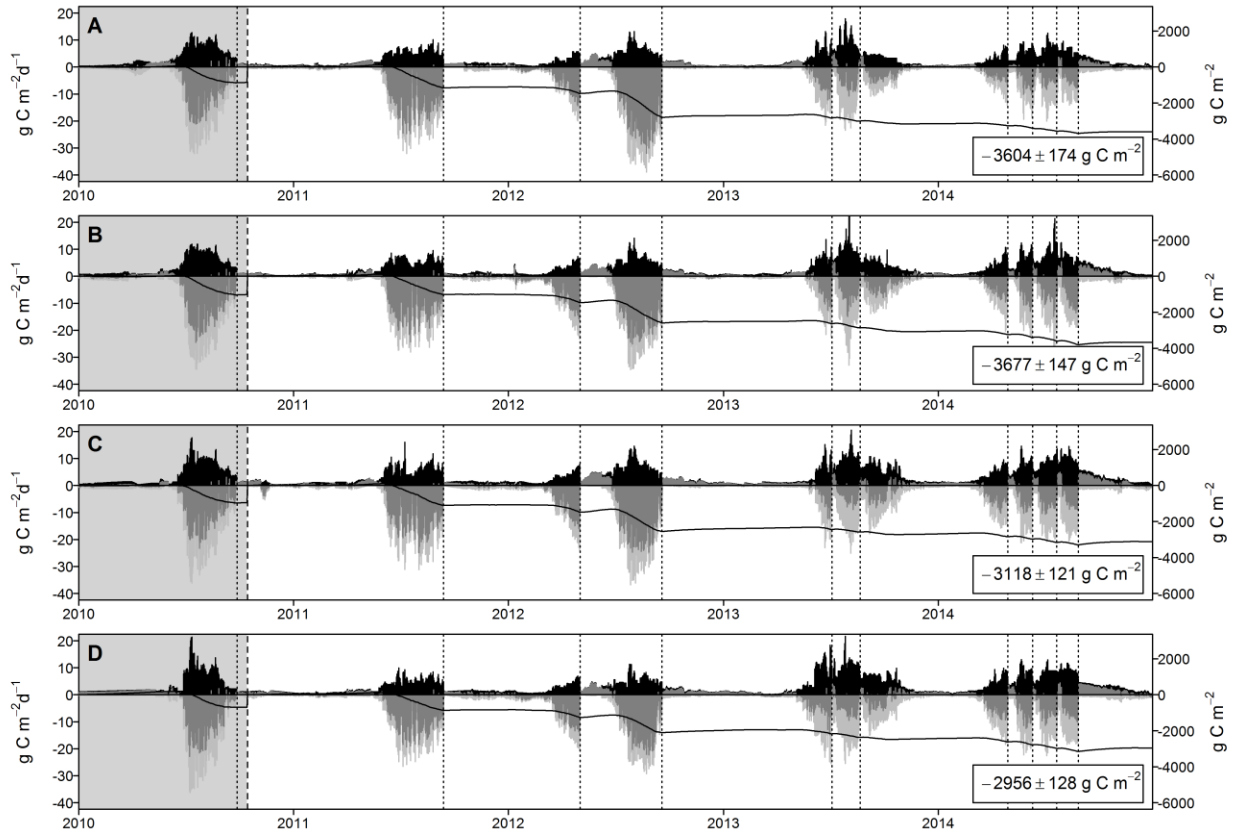
854

855

856

857

858 **Fig. 3**



859

860

861

862

863

864

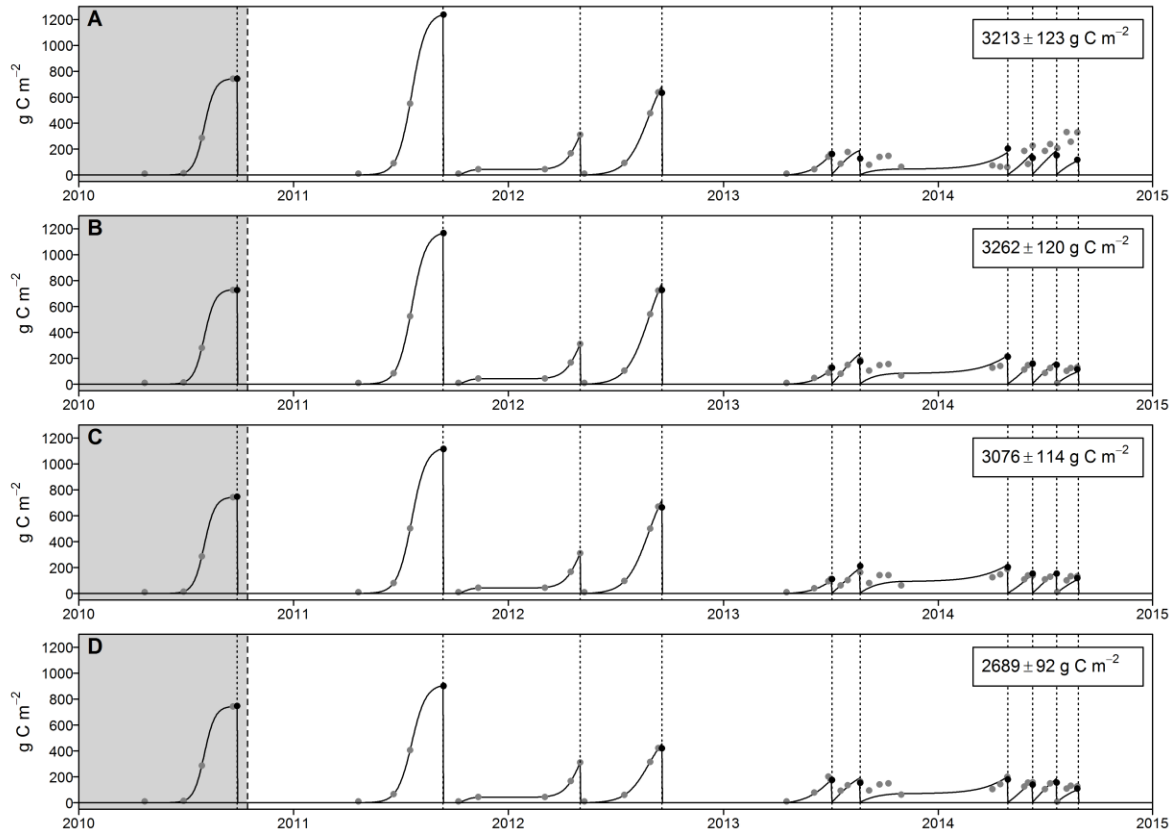
865

866

867

868

869 **Fig. 4**



870

871

872

873

874

875

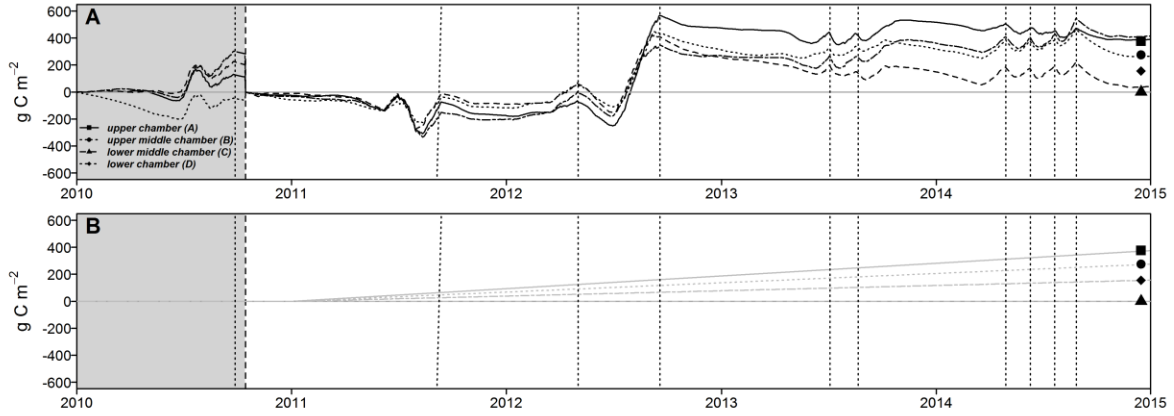
876

877

878

879

880 **Fig. 5**



881

882

883

884

885

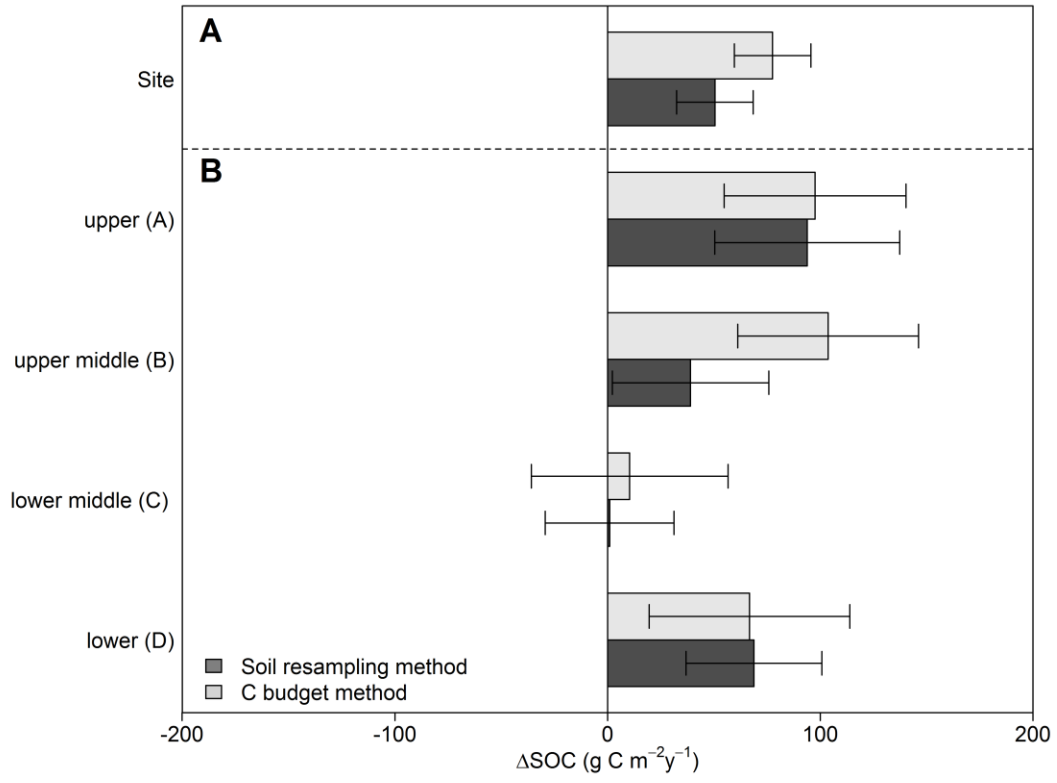
886

887

888

889

890 **Fig. 6**



891

892

893

894

895

896

897

898

899 **Appendices**900 **A.1**

Crop	Treatment	Details	Date
Winter fodder rye (<i>Secale cereale</i>)	Chamber dismounting		10/04/2010
	Herbicide application	Roundup (2 l/ha)	19/04/2010
	Fertilization	KAS (160 kg/ha N), 110 kg/ha P2O5, 190 kg/ha K2O, 22 kg/ha S and 27 kg/ha MgO	23/04/2010
	Ploughing	Chisel Plough	23/04/2010
	Sowing	10 seeds/m ²	23/04/2010
Silage maize (<i>Zea mays</i>)	Chamber installation		04/05/2010
	Herbicide application	Zintan Platin Pack	26/05/2010
	Harvest		19/09/2010
Bare soil	Chamber dismounting		20/09/2010
	Chamber installation		27/10/2010
	Chamber dismounting		05/04/2011
	Fertilization	110 kg/ha P2O5, 190 kg/ha K2O, 22 kg/ha S and 27 kg/ha MgO	06/04/2011
	Ploughing	Chisel Plough	21/04/2011
Silage maize (<i>Zea mays</i>)	Sowing	10 seeds/m ²	21/04/2011
	Herbicide application	Gardo Gold Pack, 3.5 l/ha	27/04/2011
	Fertilization	KAS (160 kg/ha N)	03/05/2011
	Chamber installation		04/05/2011
	Harvest		13/09/2011
Bare soil	Chamber dismounting		13/09/2011
	Ploughing	Chisel Plough	30/09/2011
	Sowing	270 seeds/m ²	30/09/2011
Winter fodder rye (<i>Secale cereale</i>)	Chamber installation		05/10/2011
	Fertilization	KAS (80 kg/ha N)	06/03/2012
	Harvest		02/05/2012
	Chamber dismounting		02/05/2012
Bare soil	Ploughing		08/05/2012
	Sowing	30 seeds/m ²	09/05/2012
	Fertilization	KAS (100 kg/ha N), Kieserite (100 kg/ha), 220 kg/ha P2O5, 190 kg/ha K2O	14/05/2012
Sorghum-Sudan grass (<i>Sorghum bicolor x sudanese</i>)	Chamber installation		22/05/2012
	Replanting		29/05/2012
	Herbicide application	Gardo Gold Pack (3 l/ha), Buctril (1.5 l/ha)	12/07/2012
	Harvest		18/09/2012
	Chamber dismounting		19/09/2012
Bare soil	Ploughing	Chisel Plough	09/10/2012
	Sowing	400 seeds/m ²	09/10/2012
	Chamber installation		19/10/2012
Winter triticale (<i>Triticosecale</i>)	Chamber dismounting		20/09/2012
	Chamber installation		17/10/2012
	Ploughing; fertilization	Chisel Plough; 44 kg/ha K2O, 48.4 kg/ha P40	15/04/2013
Luzerne (<i>Medicago sativa</i>)	Sowing	22 kg/ha	18/04/2013
	Harvest (first cut)		04/07/2013
	Fertilization	88 kg/ha K2O	10/07/2013
	Harvest (second cut)		21/08/2013
	Fertilization	200 kg/ha K2O, 110 kg/ha P2O5	27/02/2014
	Harvest (first cut)		29/04/2014
	Harvest (second cut)		10/06/2014
	Harvest (third cut)		21/07/2014
	Harvest (fourth cut)		27/08/2014
	Chamber dismounting		28/08/2014

901 **A.2 Weather and soil conditions**

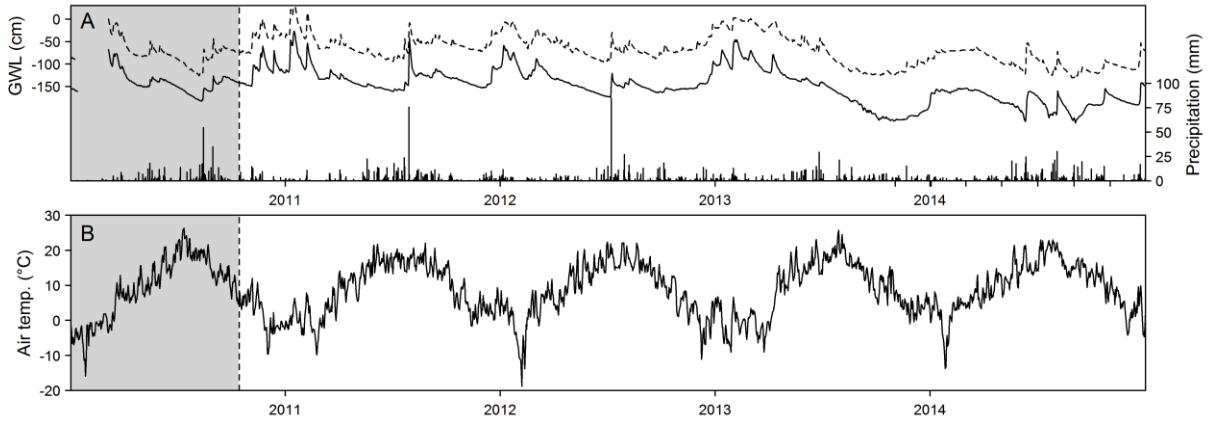
902 A.3 shows the development of important environmental variables throughout the study period
903 (January 2010 – December 2014). In general, weather condition were similarly warm (8.7°C) but
904 also wetter (562 mm) compared to the long-term average (8.6°C; 485 mm). Temperature and
905 precipitation were characterized by distinct inter- and intra-annual variability. The highest annual
906 air temperature was measured in 2014 (9°C). The highest annual precipitation was recorded
907 during 2011 (616 mm). Lower annual mean air temperature and comparatively drier weather
908 conditions were recorded in 2010 (7.7°C; 515 mm) and 2013 (8.5°C; 499 mm). Clear seasonal
909 patterns were observed for air temperature. The daily mean air temperature at a height of 200 cm
910 varied between -18.8°C in February 2012 and 26.3°C in July 2010. Rainfall was highly variable
911 and mainly occurred during the growing season (55 % to 93 %), with pronounced heavy rain
912 events during summer periods, exceeding 50 mm d⁻¹. Despite a rather wet summer, only 67 mm
913 was measured in March and April 2012, the driest spring period within the study, resulting in late
914 germination and reduced plant growth. Annual GWL differed by up to 77 cm along the chamber
915 transect and followed precipitation patterns. Seasonal dynamics were characterized by a lower
916 GWL within the growing season (1.10 m) and enhanced GWL during the non-growing season
917 (0.85 m). From a short-term perspective, GWL was closely related to single rainfall events.
918 Hence, a GWL of 0.10 m was measured immediately after a heavy rainfall event in July 2011,
919 whereas the lowest GWL occurred during the dry spring in 2010. From August 2013 to
920 December 2014, the GWL was too low to apply the principal of hydrostatic equilibrium;
921 therefore, the groundwater table depth (> 235 cm) had to be used as a proxy.

922

923

924

925 A.



926